Eur. Phys. J. E (2016) **39**: 58
DOI 10.1140/epje/i2016-16058-9

THE EUROPEAN PHYSICAL JOURNAL E

Regular Article

Effect of Gaussian curvature modulus on the shape of deformed hollow spherical objects

C. Quilliet[a], A. Farutin, and P. Marmottant

CNRS/Université Grenoble Alpes, LIPhy, F-38000 Grenoble, France

Received 22 March 2016 and Received in final form 27 April 2016
Published online: 6 June 2016 –

Abstract. A popular description of soft membranes uses the surface curvature energy introduced by Helfrich, which includes a spontaneous curvature parameter. In this paper we show how the Helfrich formula can also be of interest for a wider class of spherical elastic surfaces, namely with shear elasticity, and likely to model other deformable hollow objects. The key point is that when a stress-free state with spherical symmetry exists before subsequent deformation, its straightforwardly determined curvature ("geometrical spontaneous curvature") differs most of the time from the Helfrich spontaneous curvature parameter that should be considered in order to have the model being correctly used. Using the geometrical curvature in a set of independent parameters unveils the role of the Gaussian curvature modulus, which appears to play on the shape of an elastic surface even though this latter is closed, contrary to what happens for surfaces without spontaneous curvature. In appendices, clues are given to apply this alternative and convenient formulation of the elastic surface model to the particular case of thin spherical shells of isotropic material (TSSIMs).

Introduction

There is a recent interest, motivated by the development of fluid-related microengineering [1,2], for hollow objects with spherical symmetry (denominated here as HOSSs) undergoing deformations [3,4]. Among these objects, a sub-class is constituted by the well-known thin spherical shells *of isotropic material* or TSSIMs, that may be just referred to as "thin shells" in the literature [5].

For TSSIMs, it was shown long ago how the elastic energy can be split, with reasonable approximation, into curvature and (locally) in-plane deformation energy of a model surface [5,6]. This considerably simplifies theoretical developments and numerical treatments compared to a 3D approach where the material that forms the shell is fully modeled. In sect. 1, we will first recall how, when a TSSIM presents a stress-free reference state, 3D considerations can lead to the expression of the elastic deformation energy in a 2D surface model. Then we will extend to HOSSs the model derived for TSSIMs, with specification of the implications. In sect. 2, we still stick to the modelization of HOSSs, using instead the Helfrich model [7]. This second approach has been widely used in the field of fluid lipid membranes, and we will compare the notion of spontaneous curvature in both descriptions. In sect. 3, we detail the consequences on the role of the Gaussian curvature modulus, that surprinsingly appears to be of some importance in the shape of objects showing spontaneous curvature, though its role is nil due to topological reasons when a closed surface is symmetrical (*i.e.* without spontaneous curvature).

[a] e-mail: Catherine.Quilliet@univ-grenoble-alpes.fr

1 Deformation energy using a reference state

1.1 Thin shells of isotropic material

This subsection highlights how a concept of *geometrical* spontaneous curvature can emerge from the modelization, as a surface, of an initially stress-free thin shell of an isotropic material. Experimentally, such objects can be obtained by growing, or moulding in a template, some (isotropic) material without stress. This happens, *e.g.*, when making a commercial beach ball or some colloidal shells in suspension [8].

As detailed in appendix A, the integration of the deformations of the bulk material on the whole shell thickness leads to a more handy surface model (*i.e.* description of the shell conformation through a bidimensional object), where curvature deformations on the one hand, and tangential ("in-plane") deformations are decoupled. This appears clearly in the expression of the total deformation

energy E, as a sum of both contributions:

$$E = \iint \left[\frac{1}{2}\kappa\left(c_1+c_2-2c_S\right)^2 + \overline{\kappa}\left(c_1-c_S\right)\left(c_2-c_S\right)\right]\mathrm{d}A_{\mathrm{def}} + \iint \left[\frac{1}{2}\chi_{2\mathrm{D}}\left(\mathrm{Tr}\,\epsilon_i^j\right)^2 + \mu_{2\mathrm{D}}\left(\mathrm{Tr}\left(\left(\epsilon_i^j\right)^2\right) - \frac{1}{2}\left(\mathrm{Tr}\,\epsilon_i^j\right)^2\right)\right]\mathrm{d}A_{\mathrm{init}}, \quad (1)$$

Here c_1 and c_2 are the curvatures in the principal planes, ϵ_i^j is the in-plane deformation tensor, and $\mathrm{d}A_{\mathrm{def}}$ (respectively, $\mathrm{d}A_{\mathrm{init}}$) an infinitesimal element of the deformed (respectively, undeformed) surface. The parameter c_S, denominated in appendix A as the *geometrical* spontaneous curvature, is the curvature in any principal plane of the initial (stress-free) spherical conformation (in others terms it is the inverse of the initial radius R).

The prefactor κ (respectively, $\overline{\kappa}$, $\chi_{2\mathrm{D}}$, $\mu_{2\mathrm{D}}$) is the mean curvature (respectively, Gaussian curvature, 2D stretch, 2D shear) elastic modulus. Calculations show that these moduli associated to the model surface can be expressed using the features of the material shell (namely its thickness d plus a pair of parameters to account for the elasticity of a bulk isotropic material, *e.g.* Young modulus and Poisson's ratio ($Y_{3\mathrm{D}}, \nu_{3\mathrm{D}}$), or 3D stretch and shear moduli ($\chi_{3\mathrm{D}}, \mu_{3\mathrm{D}}$)). Moreover, the main dependence of 2D moduli on the 3D features is the same as for thin plates [5] —and it is recalled for the four of them in eqs. (A.5) and (A.6) of appendix A. From these relations it can be deduced that the quantity $(1+\frac{\overline{\kappa}}{\kappa})$ has to be equal to the bulk Poisson's ratio $\nu_{3\mathrm{D}}$, which is thermodynamically restricted to the interval $[-1, \frac{1}{2}]$. Hence the condition on (2D) curvature moduli for the description of a TSSIM follows:

$$-2 \leq \frac{\overline{\kappa}}{\kappa} \leq -\frac{1}{2}\,. \quad (2)$$

In the same spirit, the equality $\frac{\chi_{2\mathrm{D}}-\mu_{2\mathrm{D}}}{\chi_{2\mathrm{D}}+\mu_{2\mathrm{D}}} = \nu_{2\mathrm{D}} = \nu_{3\mathrm{D}}$ imposes, again for the bidimensional parameters modeling a thin shell of an isotropic material:

$$\chi_{2\mathrm{D}} \leq 3\mu_{2\mathrm{D}}\,. \quad (3)$$

Lastly, the requirement that, for a thin shell, the thickness has to be much smaller than its radius, sets the condition:

$$\sqrt{12\kappa/\left(\chi_{2\mathrm{D}}+\mu_{2\mathrm{D}}\right)} \ll R. \quad (4)$$

1.2 Multilayered capsules

Although calculations leading to eqs. (A.1) and (A.4) of appendix A, and hence to eq. (1), were done for thin shells of isotropic materials, they all result from the energetic contribution of in-plane deformation of infinitely thin layers, summed on the whole plate thickness [5]. An analogous calculation could then be done on a shell formed by non-similar superimposed layers [9] (also called "multiwall capsules" [10]), as sketched in fig. 1a: after summation, its energy would take the same form as eq. (1), with 2D effective parameters that would result from the contribution of each layer. The difference is that each layer cannot be considered as free from tangential constraints at their boundaries, therefore relations (A.5) and (A.6) of appendix A (that were resulting from these precise hypotheses) do not hold any more, nor their sequels eqs. (2), (3) and (4). For what concerns the 2D parameters qualifying the model surface of such object, the only restriction is then the general one in 2D elasticity, *i.e.* the Poisson's ratio $\nu_{2\mathrm{D}} = \frac{\chi_{2\mathrm{D}}-\mu_{2\mathrm{D}}}{\chi_{2\mathrm{D}}+\mu_{2\mathrm{D}}}$ belonging to the interval $[1, -1]$ (imposed by $\chi_{2\mathrm{D}}$ and $\mu_{2\mathrm{D}}$ being non-negative, as demonstrated *e.g.* in [11]).

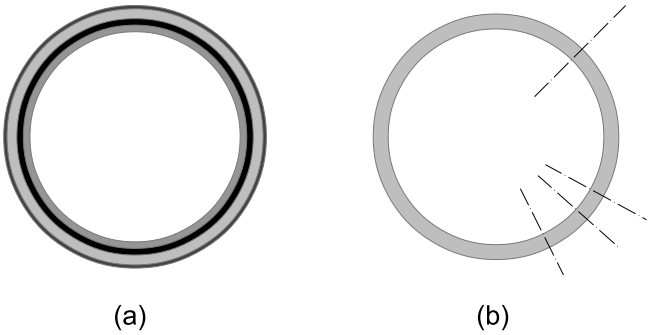

Fig. 1. Examples of shells that are not made of a single isotropic material, and nevertheless compatible with the symmetry of an isotropic model surface. (a) Multiwall capsule, made of superimposed layers of different isotropic materials. (b) Shell made of a transversely isotropic material (*i.e.* uniaxal anisotropic material) with its symmetry axis being radial on the whole shell.

1.3 Other types of hollow objects with spherical symmetry

More generally, an isotropic elastic surface with an energy of the form given by eq. (1) is expected to model the deformation of spherical shells made of any material, *i.e.* possibly heterogeneous or anisotropic, as long as, at the scale of interest, their symmetries are compatible with the 2D isotropy and homogeneity of the model surface (which was summarized in the introduction by the acronym HOSS). Beside layered materials, uniaxial anisotropic materials (also called *transversely isotropic materials*) also fulfill these requirements, when before deformation their symmetry axis is radial on the whole spherical shell (fig. 1b). When the surface model proves to be efficient to retrieve experimental shapes, the key clue is to establish relations between the 2D parameters, and the 3D specificities of the thin shell (geometry and material properties). This was done successfully on "solid" (*i.e.* with shear elasticity) lipid vesicles deflated by osmotic pressure [12], vesicles being shells whose *transversely* isotropic material is the (possibly fluctuating) phospholipid membrane.

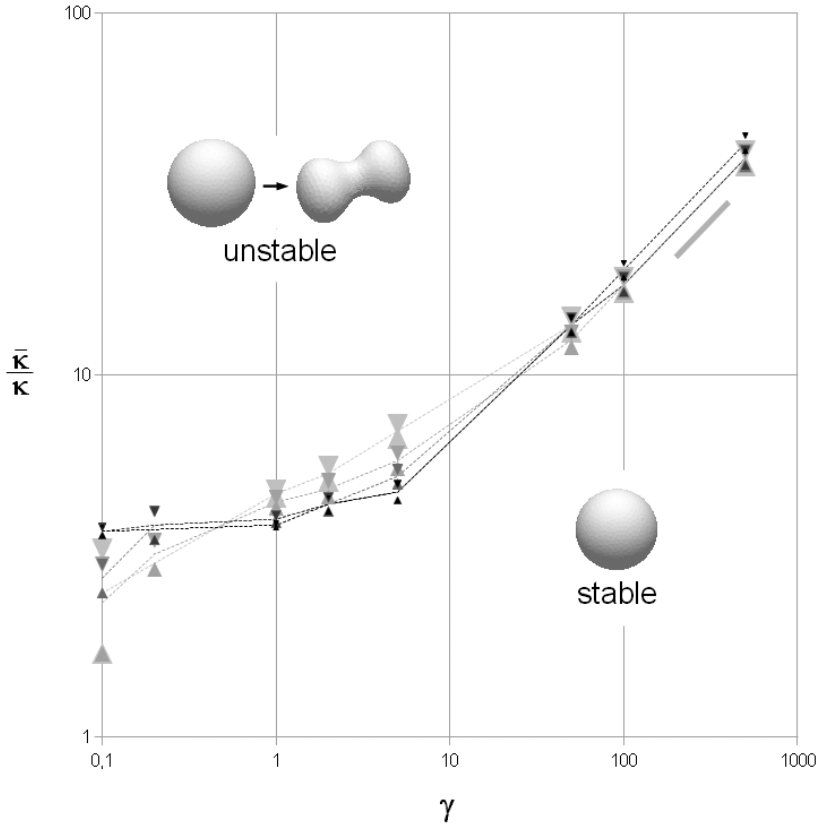

Fig. 2. Stability diagram of the initial stress-free spherical surface whose deformation energy is provided by eq. (1) (scanned under its more convenient form (5) derived in sect. 2; minimizations are performed using the free software Surface Evolver [13]). Horizontal axis: Föppl-von Karmán number γ [14]. This latter adimensionalizes the 2D Young modulus Y_{2D}: $\gamma = \frac{Y_{2D}R^2}{\kappa} = \frac{4\chi_{2D}\mu_{2D}R^2}{\kappa(\chi_{2D}+\mu_{2D})}$. From darker to lighter and with increasing size, the points correspond to Poisson's ratios $\nu_{2D} = \frac{\chi_{2D}-\mu_{2D}}{\chi_{2D}+\mu_{2D}}$: -0.8, -0.5, 0, $+0.5$ and $+0.8$. Upward (respectively, downwards) triangles: highest (respectively, lowest) value of $\kappa/\overline{\kappa}$ for which the sphere conformation was stable (respectively, unstable). Broken lines with corresponding shades of grey join the average values. Short thick grey line indicates the slope 0.5. The example shown in the unstable zone is taken just above the border: $\gamma = 5$, $\nu = 0.8$ and $\kappa/\overline{\kappa} = 6.5$; in the non-spherical stable conformation the volume decreases by 34%.

1.4 Stability of the surface model

As shown in appendix B, the elastic deformation energy per surface unit $e_{\rm el}$, which is the sum of curvature deformation energy $e_{\rm curv}$ (eq. (A.1) of appendix A) and tangential deformation energy $e_{\text{in-plane}}$ (eq. (A.4) of appendix A), can be written as a quadratic form, which is definite positive for $-2\kappa < \overline{\kappa} < 0$[1].

Out of this range, the physical occurrence of the initial stress-free spherical conformation (that may be either stable or unstable) is not ensured. For a closed surface, topological constraints are expected to reduce the degrees of freedom of the problem, but even in this case stability is difficult to grasp analytically. Hence we performed simulations using the finite elements software Surface Evolver [13], which allows to assign the different terms of eq. (5) to the energy to be minimized. Results are summarized in fig. 2 as a $(\gamma, \frac{\overline{\kappa}}{\kappa})$ stability diagram. The limit case where $\nu \lesssim 1$ and $\gamma \ll 1$ corresponds to an incompressible surface solely driven by curvature, which is the classical model for fluid-phase vesicles of phospholipids. More generally, the range of $\overline{\kappa}/\kappa$'s for which the initial sphere is stable increases with γ, making obvious the stabilizing role of in-plane deformation energy.

Simulations were also performed at constant enclosed volume (not shown). As expected, this stabilises the initial spherical situation, but only to a small extent (not more than a few percent in $\overline{\kappa}/\kappa$).

[1] This includes in particular the case of thin plates or shells of isotropic material, for which $-2\kappa < \overline{\kappa} < -\kappa/2$.

2 Comparison with Helfrich's approach

The bending energy per surface unit expressed in (1) can be rewritten as

$$\frac{1}{2}\kappa\left(c_1+c_2-2c_S\right)^2+\overline{\kappa}\left(c_1-c_S\right)\left(c_2-c_S\right)=$$
$$\frac{1}{2}\kappa\left(c_1+c_2-2c_S\left(1+\frac{\overline{\kappa}}{2\kappa}\right)\right)^2+\overline{\kappa}c_1c_2-\overline{\kappa}c_S^2\left(1+\frac{\overline{\kappa}}{2\kappa}\right),$$

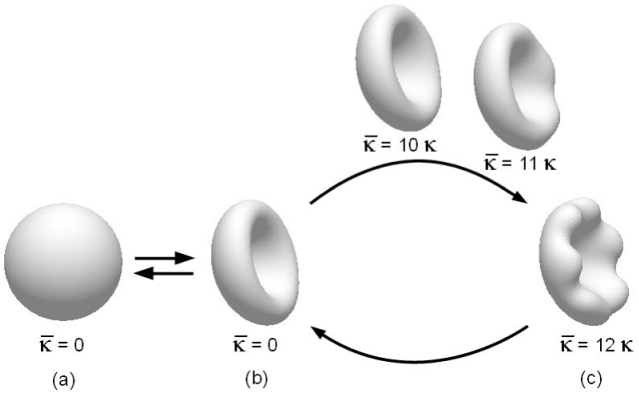

Fig. 3. Deformation of a stress-free spherical elastic surface of radius R (a) with dimensionless elastic parameters $\gamma = 121$ and $\nu_{2D} = 0.5$. Simulations use minimization of eq. (5) with Surface Evolver [13], imposing $c_S = \frac{1}{R}$ due to the stress-free nature of the initial state. From (a) to (b), $\overline{\kappa} = 0$ and the volume enclosed is slowly decreased from V_0 to $V_0/2$, leading to a buckled axisymmetric shape [20]. Between (b) and (c), $\overline{\kappa}$ is increased stepwise while all other parameters are kept unchanged (χ_{2D}, μ_{2D}, κ, c_S, volume). Decreasing $\overline{\kappa}$ back to 0 reversively provides axisymmetric shape and elastic energy of (b) with 0.5% accuracy, and (a) again after re-inflation. Mesh comprises 5948 vertices; all subfigures are represented at the same scale.

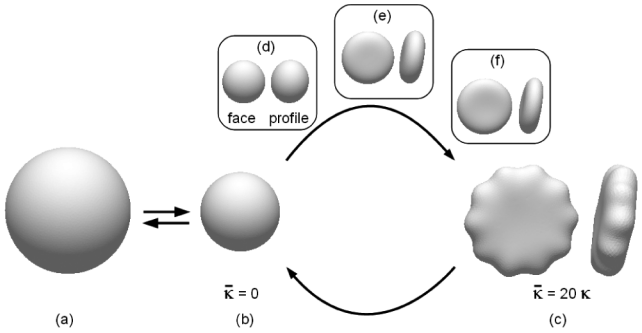

Fig. 4. The spherical stress-free elastic surface (a), here of dimensionless elastic parameters $\gamma = 20$ and $\nu_{2D} = 0.8$, deflates stepwise [20] into sphere (a). Subsequent stepwise increase of $\overline{\kappa}$ while keeping all other independent parameters constant (χ_{2D}, μ_{2D} κ, $c_S = \frac{1}{R}$, volume $V_0/3$ where V_0 is the volume enclosed in the initial state) reversibly leads to shape (c), for which $\overline{\kappa} = 20\kappa$. Decreasing $\overline{\kappa}$ back to 0 reversively provides spherical shape (b) with its initial elastic energy, and (a) again after re-inflation. Intermediate shapes are obtained for $\overline{\kappa} = 5\kappa$ (d), 10κ (e) and 15κ (f). As shown in fig. 2 and discussed in subsect. 1.4, surfaces for which $\overline{\kappa}/\kappa = 10$, 15 and 20 would not provide spheres when their inner volume were re-inflated to V_0; their conformations nevertheless unambiguously show a crucial role of $\overline{\kappa}$. Mesh comprises here 4644 vertices. Subfigures (a), (b) and (c) have the same scale, while (d), (e) and (f) are reduced (same factor).

where c_1+c_2 is the total curvature[2], and c_1c_2 is the Gauss curvature.

The Gauss-Bonnet theorem states that the integral of $\overline{\kappa}c_1c_2$ is a constant for closed C^2 surfaces (*i.e.* differentiable, *and* where a finite curvature can be defined everywhere, which is not the case *e.g.* in spherocylinders of [15]) that do not undergo a topological change; thus this term does not play a role in deformations without material breaking and we can rewrite the total energy in a form where the first term is very close to the energy proposed by W. Helfrich [7] in 1973 for the curvature of soft closed membranes:

$$E = \mathrm{cst} + \iint \left[\frac{1}{2}\kappa\left(c_1 + c_2 - 2c_0\right)^2 + \gamma_{\mathrm{eff}}\right] \mathrm{d}A_{\mathrm{def}} + \iint \left[\frac{1}{2}\chi_{2D}\left(\mathrm{Tr}\,\epsilon_i^j\right)^2 + \mu_{2D}\left(\mathrm{Tr}\left(\left(\epsilon_i^j\right)^2\right) - \frac{1}{2}\left(\mathrm{Tr}\,\epsilon_i^j\right)^2\right)\right] \mathrm{d}A_{\mathrm{init}}. \quad (5)$$

The two parameters c_0 ("Helfrich spontaneous curvature") and γ_{eff} ("effective tension") are defined as

$$c_0 = c_S\left(1 + \frac{\overline{\kappa}}{2\kappa}\right), \quad (6)$$

$$\gamma_{\mathrm{eff}} = -\overline{\kappa}c_S^2\left(1 + \frac{\overline{\kappa}}{2\kappa}\right). \quad (7)$$

[2] In the vesicles community, $c_1 + c_2$ is called "mean curvature". Since some mathematicians and mechanics specialists compute $\frac{1}{2}(c_1 + c_2)$ for the same term, we will prevent ambiguity by using the term "total curvature" for $c_1 + c_2$.

The curvature term is much more easy to compute in this description than under the form (1), since both c_1c_2 and powers of $c_1 + c_2$ can be easily integrated on triangulated surfaces (see, *e.g.*, ref. [16] or [13]) without having to determine separately c_1 and c_2. Numerical simulations of figs. 2, 3 and 4 were computed using this expression (5).

Remark:

For a closed surface, the only additional term of eq. (5) compared to the Helfrich formulation is the effective negative surface tension γ_{eff}. Actually this term can be "absorbed" in the deformation energy by introducing a new reference area for the in-plane compression energy. With this new reference state, plus reducing our purpose to closed C^2 surfaces, eq. (5) becomes

$$E = \iint \left[\frac{1}{2}\kappa\left(c_1 + c_2 - 2c_0\right)^2\right] \mathrm{d}A_{\mathrm{def}} + \iint \left[\frac{1}{2}\chi_{2D}\left(\mathrm{Tr}\,\epsilon_i^{j0}\right)^2 + \mu_{2D}\left(\mathrm{Tr}\left(\left(\epsilon_i^{j0}\right)^2\right) - \frac{1}{2}\left(\mathrm{Tr}\,\epsilon_i^{j0}\right)^2\right)\right] \mathrm{d}A_{\mathrm{init}} + \mathrm{cst}, \quad (8)$$

where we introduce the in-plane deformation tensor $\epsilon_i^{j0} = \epsilon_i^j + \frac{1}{2}\left(\frac{A_S - A_0}{A_S}\right)\delta_i^j$ that is relative to a new reference surface of area A_0 instead of $A_S = 4\pi R^2$, and where δ_i^j is the Kronecker symbol. The area change after deformation is

$\iint \mathrm{Tr}(\epsilon_i^{j0})\mathrm{d}A_{\mathrm{init}} = A - A_0$ instead of $\iint \mathrm{Tr}(\epsilon_i^{j})\mathrm{d}A_{\mathrm{init}} = A - A_S$. The surface tension term vanishes for an area A_0 chosen so that $\gamma_{\mathrm{eff}} = \chi_{2\mathrm{D}}\frac{A_S - A_0}{A_S}$. Using eq. (7), it means that the new reference area is $A_0 = A_S[1 + \frac{\overline{\kappa}c_S^2}{\chi_{2\mathrm{D}}}(1 + \frac{\overline{\kappa}}{2\kappa})]$.

Here we can notice that fluid lipid vesicles, for which the Helfrich energy was extensively used [17], can be modeled using this description by setting $\mu_{2\mathrm{D}} = 0$. For this case, the difference in the choice of the reference areas for either approaches can be neglected as long as $|\overline{\kappa}|c_S^2/\chi_{2\mathrm{D}} \ll 1$, which is always the case in lipid vesicles (typically $\chi_{2\mathrm{D}} \approx 250\,\mathrm{mN/m}$, and $|\overline{\kappa}|$ can be assumed as not exceeding the order of magnitude of $\kappa \approx 15\,kT$; inequality then corresponds to $1/c_S \gg 5 \cdot 10^{-10}\,\mathrm{m}$, which is smaller than the bilayer thickness). Consequently, in-plane deformation does not occur in practice for vesicles bigger than $\sqrt{\kappa/\chi_{2\mathrm{D}}} \approx$ a few nm (which allows to safely ignore the γ_{eff} term in the first approach), and even in this limit it would not affect the dimensionless equilibrium shape [18].

3 Role of the Gaussian curvature elasticity

A fundamental consequence of previous considerations is that, contrary to what is commonly maintained in capsules or vesicles physics, the Gaussian curvature modulus $\overline{\kappa}$ is expected to play a role on the shape after deformation, despite the vanishing of the $\overline{\kappa}c_1c_2$ term on closed C^2 surfaces due to the Gauss-Bonnet theorem. Indeed the Helfrich spontaneous curvature c_0 depends on $\overline{\kappa}$, which explicitly appears when using the predictable parameter c_S (eq. (6)). In order to look for the effectiveness of this remark, we numerically studied the equilibrium shape of initially spherical isotropic surfaces, deflating them and studying the influence of $\overline{\kappa}$ by varying its value while keeping all the other parameters (c_S, κ, $\chi_{2\mathrm{D}}$, $\mu_{2\mathrm{D}}$) unchanged.

For these simulations, using sets of 2D parameters that correspond to thin shells of isotropic materials would have allowed to add intuitive knowledge to calculations, since most of us (authors and readers) played with TSSIM's many times, *e.g.* as beach balls. But in the special case of TSSIM's, 2D parameters are bound in such a way (see eqs. (A.5) and (A.6) of appendix A) that when c_S, κ, $\chi_{2\mathrm{D}}$, $\mu_{2\mathrm{D}}$ are kept unchanged, $\overline{\kappa} = -2\mu_{2\mathrm{D}}/(\chi_{2\mathrm{D}} + \mu_{2\mathrm{D}})$ cannot be varied. We had then to use sets of 2D parameters that go beyond the specificities corresponding to thin shells of an isotropic material. Performing such simulations, we could observe that the role of the sole $\overline{\kappa}$ may be far from negligible. Figure 3 shows that an axisymmetric deflated shape may show destabilization of its rim when $\overline{\kappa}$ increases while all other parameters (inner volume, $\chi_{2\mathrm{D}}$, $\mu_{2\mathrm{D}}$ κ, $c_S = \frac{1}{R}$) are kept constant. Indeed, bumps of shape (c) are favoured for high $\overline{\kappa}$'s by the strongly positive value of $c_0 = c_S(1 + \frac{\overline{\kappa}}{2\kappa}) \gg R^{-1}$ [19,18], and by the negative value of $\gamma_{\mathrm{eff}} = -\overline{\kappa}c_Sc_0$ that plays in favor of surface increase.

It is possible to observe even more striking effects of $\overline{\kappa}$, for sets of elastic parameters that correspond to the unstable zone of fig. 2[3]. In these simulations, presented in fig. 4, a stable sphere at $\overline{\kappa} = 0$ is deflated without losing its spherical symmetry, and then only $\overline{\kappa}$ is altered. Even for high Gaussian curvature moduli, stable equilibrium shapes are obtained. The striking consequence of such a drastic increase of $\overline{\kappa}$ is not only the appearance of scallop-squash-like festoons, but, first, a general flattening of the reduced sphere. This unambiguously shows the role and importance of the Gaussian curvature modulus $\overline{\kappa}$.

4 Discussion

Successfully modeling the deformation of a hollow object with an elastic surface immediately raises this issue: how does the 2D parameters connect with the 3D features of the object? The answer being strongly entangled with the object's geometry, we restricted here our purpose to hollow objects with a spherical symmetry (HOSSs). Following previous approaches [6,5,21], we derived the 3D materials deformation in order to obtain two energetic contributions related to the deformation of an isotropic solid (*i.e.* with shear energy cost) *surface*, one dealing with tangential deformations (stretch, shear) and one concerned with curvature deformations, for which a Helfrich form can be used following what was successfully done in the community of lipid fluid vesicles. In the situation where the HOSS has a stress-free reference state, we showed how to correctly use the Helfrich curvature form when the spontaneous curvature parameter c_0 (devoted to the description of naturally bend, or "asymmetric", surfaces) is non-zero. Through eqs. (5), (6) and (7), we could establish the correspondence between *a priori* determinable parameters (curvature moduli κ and $\bar{\kappa}$, and curvature c_S in the reference, or "initial", state), and the heuristic parameter c_0 that can be obtained from comparisons between experimental and theoretical shapes (see *e.g.* framework in [22] and references herein for c_0 to be used in fluid vesicles, which is the limit case of solid vesicles where $\mu_{2\mathrm{D}} \ll \chi_{2\mathrm{D}}$). Application is shown in appendix C for the description of a thin spherical shell of an isotropic material (TSSIM).

In the general case for HOSSs, we can note that the Helfrich spontaneous curvature c_0 is clearly *effective*, as discussed in [23]. This parameter is known for long to be of utmost importance for the shape of vesicles, and in this paper it appears as summing up the influences of c_S and $\overline{\kappa}$ in closed surfaces. The geometrical spontaneous curvature c_S can be determined, either because the stress-free reference state is accessible, either through independent micro- or mesoscopic considerations such as the packing parameter in the surfactant monolayers that build microemulsions [24], or meniscus calculations between the solid particles that stabilize the interface in Pickering emulsions [23,

[3] Such parameters are not "unphysical", they just correspond to situations where the constraint-free spherical conformation is unstable. Interestingly, as it is shown in fig. 2, deflation may bring stability to a closed surface, that would be unstable without volume constraints. On such systems the effect of high values of $\overline{\kappa}$ is clearly first-order.

25]. Besides, due to various technical performances, experimental 3D shapes are determined nowadays with increasing precision [17]. Hence comparing experimental shapes with the theoretical ones —obtained *e.g.* using eq. (5)— allows a determination of c_0 that leads, with knowledge of c_S, to $\overline{\kappa}$. This latter, not easily obtainable through other considerations in the absence of free edges, was not taken into account in most of the preeceding studies; the results presented in this paper prove the up to now underestimated importance of the Gaussian curvature modulus $\overline{\kappa}$ in the shape of closed objects.

Authors thank C. Misbah for fruitful discussions, and are greatly indebted to the conception and support of Surface Evolver by K. Brakke.

Appendix A. Obtention of a 2D surface model for a thin shell made of an isotropic material

The deformation from a stress-free curved reference state of a thin layer of isotropic material ("shell") has been derived by Niordson [26] and extensively used in ref. [21], allowing its description with a mathematical surface described by the vector $\mathbf{r}(s^1, s^2)$, in which s^1 and s^2 serve as coordinates. Though this is not necessary for curvature considerations, we will consider that a pair of coordinates (s^1, s^2) holds for the same material point in the initial and deformed situation: this allows us to have a Lagrangian approach for the subsequent treatment of in-plane deformations. Through integration of the 3D deformation energy (neo-Hookean elasticity) in the whole shell thickness, one can write the main order terms for the curvature energy per surface unit:

$$e_{\text{curv}} = \frac{1}{2}\kappa\left(\text{Tr}\left(c_i^j - C_i^j\right)\right)^2 + \overline{\kappa}\det\left(c_i^j - C_i^j\right), \quad \text{(A.1)}$$

where c_i^j is defined by $c_i^j = h_{ik}g^{kj}$ (respectively, $C_i^j = H_{ik}G^{kj}$), with h_{ij} (respectively, H_{ij}) being the second fundamental tensor of the deformed (respectively, undeformed) surface, and g^{ij} (respectively, G^{kj}) is the inverse of the metric tensor of the deformed (respectively, undeformed) surface:

$$h_{ij} = \mathbf{n}\cdot\frac{\partial^2\mathbf{r}}{\partial s^i \partial s^j}, \quad \text{(A.2)}$$

$$g^{ij} = (g_{ij})^{-1} = \left(\frac{\partial\mathbf{r}}{\partial s^i}\cdot\frac{\partial\mathbf{r}}{\partial s^j}\right)^{-1}. \quad \text{(A.3)}$$

The vector $\mathbf{n} = (\frac{\partial\mathbf{r}}{\partial s^1}\times\frac{\partial\mathbf{r}}{\partial s^2})/\|\frac{\partial\mathbf{r}}{\partial s^1}\times\frac{\partial\mathbf{r}}{\partial s^2}\|$ is the unit normal. These tensors are such that $\text{Tr}(c_i^j)$ (respectively, $\text{Tr}(C_i^j)$) is the total curvature (see note 2 of main text) of the deformed (respectively, undeformed) surface, while $\det(c_i^j)$ (respectively, $\det(C_i^j)$) is its Gaussian curvature. In the following, we will call c_i^j (respectively, C_i^j) the *curvature tensor* of the deformed (respectively, undeformed) undeformed surface[4].

Detailed calculation by Niordson show that the prefactors κ and $\overline{\kappa}$ are, respectively, the same bending and Gaussian curvature moduli than for plane thin layers ("thin plates") of similar thickness and material, that are displayed in eq. (A.6)[5].

For an isotropic spherical surface, C_i^j is an isotropic tensor

$$C_i^j = c_S\delta_i^j,$$

where $c_S = 1/R$, called the *geometrical* spontaneous curvature, is the inverse of the radius of the initial stress-free spherical surface. In this particuliar but ubiquitous case, and with c_1 and c_2 being the curvatures in the principal planes, we get

$$\text{Tr}\left(c_i^j - C_i^j\right) = \text{Tr}\left(c_i^j\right) - \text{Tr}\left(C_i^j\right) = c_1 + c_2 - 2c_S,$$
$$\det\left(c_i^j - C_i^j\right) = (c_1 - c_S)(c_2 - c_S).$$

The other contribution obtained from the integration of the deformation energy in the shell thickness amounts at leading order to "in-plane" (2D) deformation energy per surface unit [26,21]

$$e_{\text{in-plane}} = \frac{1}{2}\chi_{2\text{D}}\left(\text{Tr}\,\epsilon_i^j\right)^2 + \mu_{2\text{D}}\left(\text{Tr}\left((\epsilon_i^j)^2\right) - \frac{1}{2}\left(\text{Tr}\,\epsilon_i^j\right)^2\right), \quad \text{(A.4)}$$

where $\chi_{2\text{D}}$ is the compression modulus (for equal compressions of the surface along the principal axis), $\mu_{2\text{D}}$ is the shear modulus (linked to elongations with opposite values along the principal axis), and ϵ_i^j is a 2D deformation

[4] Equation (A.1) is slightly different from eq. (25) of ref. [21] due to the definition of c_i^j and C_i^j. For what concerns the definition of the mixed bending tensor that quantifies curvature deformations, ref. [26] explains that selecting the difference between the undeformed and deformed state for either the covariant components $(h_{ik} - H_{ik})g^{kj}$ or the mixed components $(h_{ik}g^{kj} - H_{ik}G^{kj})$ only affects higher-order terms in the deformation energy. Hence we chose here the second option through a definition of the bending tensor as $h_{ik}g^{kj} - H_{ik}G^{kj} = c_i^j - C_i^j$, which allows an explicit role of the principal curvature radii of the undeformed and deformed surfaces in the deformation energy. Another divergence is that refs. [26] and [21] denominate h_{ij} as the "curvature tensor". We chose not to follow this second nomenclature, potentially deceptive since h_{ij} has the dimension of a total curvature (*i.e.* inverse of a length) only when coordinates s^i are lengths. So we will keep this denomination of "curvature tensor" for the mixed tensors $c_i^j = h_{ik}g^{kj}$ and $C_i^j = H_{ik}G^{kj}$.

[5] There may also be discrepancies between different communities about the definition of κ. Here we used the definition that rules in the Soft Matter community, and more particularly in the physics of lipids vesicles, where κ is such that the bending energy of a spherical surface without spontaneous curvature is $8\pi\kappa$.

tensor. Calculations show that both moduli are, at leading order, the same as for thin plates with zero tangential constraints at their upper and lower boundaries [5].

The first important consequence is that the 3D deformations of the shell can be decoupled, using an elastic isotropic surface model, into 2D elasticity on the one hand, plus (total and Gaussian) curvature elasticity on the other hand. Both contributions have to be integrated on the whole object. Following what is done in physics of curved membranes, we chose to integrate the curvature energy $e_{\rm curv}$ on the deformed surface. The advantage is that adimensionalizing an infinitesimal element of the deformed surface $\mathrm{d}A_{\rm def}$ with a squared total curvature, or a Gaussian curvature, provides the angles that accounts for local deformation independently from scale (hence from possible in-plane deformations), which is not the case with an infinitesimal element of the undeformed (initial) surface $\mathrm{d}A_{\rm init}$. With regard to $e_{\text{in-plane}}$: in a linear model treating small deformations, integration can be performed either on deformed or on undeformed surface. In order to cover a larger spectrum of deformations, we adopted the adimensioned surface Lagrangian finite strain tensor [27] $\epsilon_i^j = \frac{1}{2}(g_{ik}G^{kj} - \delta_i^j)$ and integrated in on the undeformed surface.

In summary, summing both curvature and 2D deformation energies leads to the (main text) expressions (1) and/or (5) for the total deformation energy, where the 2D parameters characterizing the model surface can be explicited using 3D features (thickness d of the shell, Young modulus $Y_{\rm 3D}$ and Poisson's ratio $\nu_{\rm 3D}$ of its isotropic bulk material):

$$\mu_{\rm 2D} = \frac{Y_{\rm 3D} d}{2(1+\nu_{\rm 3D})}\,; \qquad \chi_{\rm 2D} = \frac{Y_{\rm 3D} d}{2(1-\nu_{\rm 3D})} \tag{A.5}$$

$$\kappa = \frac{Y_{\rm 3D}}{12(1-\nu_{\rm 3D}^2)}\, d^3;$$

$$\overline{\kappa} = (\nu_{\rm 3D} - 1)\,\kappa = -\frac{Y_{\rm 3D}}{12(1+\nu_{\rm 3D})}\, d^3. \tag{A.6}$$

Appendix B. Comparison between curvature and in-plane deformation energies; interpretation of $\overline{\kappa}$

The curvature part of the energy expressed in eq. (1) can be re-written as a quadratic form

$$e_{\rm curv} = \frac{1}{2}\left(\kappa + \frac{1}{2}\bar{\kappa}\right)(c_1 + c_2 - 2c_S)^2 - \frac{1}{4}\bar{\kappa}\,(c_1 - c_2)^2\,. \tag{B.1}$$

Obviously, this form is definite positive, and hence the curvature energy of an elementary surface is stable, if $-2\kappa < \overline{\kappa} < 0$ (contrary to κ, $\overline{\kappa}$ can take negative values). In this formulation, $-\frac{1}{2}\bar{\kappa}$ in the second term can be seen as the modulus linked to the cost of non-isotropic curvatures (such that $c_1 \neq c_2$). The first term is obviously linked to the cost of total curvature away from c_S, with a modulus $\kappa + \frac{1}{2}\bar{\kappa}$.

A parallel can be drawn with the in-plane deformation energy that writes

$$e_{\text{in-plane}} = \frac{1}{2}\chi_{\rm 2D}\,(\epsilon_1 + \epsilon_2)^2 + \frac{1}{2}\mu_{\rm 2D}\,(\epsilon_1 - \epsilon_2)^2\,, \tag{B.2}$$

with ϵ_1 and ϵ_2 the eigenvalues of the deformation tensor. There is a formal analogy between the two energies, one computed from the tensor $c_i^j - C_i^j$ (cf. appendix A) and the other from the tensor ϵ_i^j. Non-isotropic curvature gives rise to an energy with a modulus $-\frac{1}{2}\bar{\kappa}$ for eq. (B.1), and similarly non-isotropic in-plane deformation gives rise to an energy with a prefactor $\mu_{\rm 2D}$.

Equation (B.2) then provides another interpretation of the physical meaning of the Gauss curvature modulus $\bar{\kappa}$, which is the consequence of non-isotropic curvatures.

Appendix C. Helfrich approach applied to thin shells made of an isotropic material

Applying relations (6) and (7) to a thin shell of an isotropic material (TSSIM), which can be modeled by a surface with 2D parameters covered by eqs. (A.5) and (A.6), leads to

$$\gamma_{\rm eff} = \frac{1+\nu_{\rm 3D}}{2\,R^2}\,\kappa; \qquad c_0 = \frac{1+\nu_{\rm 3D}}{2\,R}\,\kappa. \tag{C.1}$$

The second relation clearly reminds that c_0 is not a geometric quantity like $c_S = 1/R$, but indeed a parameter that also takes into account elastic features (here $\nu_{\rm 3D}$), and that can vary between 0 and $\frac{3}{2R}$ on the whole range of accessible Poisson's ratios. This approach allowed computation of shapes of deflated TSSIMs in ref. [20].

Domain of validity

From the discussion at the end of sect. 2, we infer that modelling a thin spherical shell of an isotropic material (TSSIM) of thickness d with a spherical elastic surface of radius R requires $|\overline{\kappa}|c_S^2/\chi_S \ll 1$ (with $c_S = 1/R$), which amounts to $(\frac{d}{R})^2 \ll 6\,\frac{1+\nu_{\rm 3D}}{1-\nu_{\rm 3D}}$. This is always the case for thin shells as long as the material is not unusually auxetic (auxeticity qualifies materials where $\nu_{\rm 3D} < 0$, the lower limit being, as for all solids, $\nu_{\rm 3D} = -1$).

The full form to be used for a deformed spherical shell then writes, after replacing the parameters of eqs. (A.5), (A.6) above in eq. (5):

$$E_{\rm sph.TSIM} = 4\pi\overline{\kappa} + \frac{Y_{\rm 3D} d^3}{12(1-\nu_{\rm 3D}^2)} \times \left\{ \iint \left[\frac{1}{2}\left(c_1 + c_2 - 2\frac{1+\nu_{\rm 3D}}{2R}\right)^2 - \frac{1+\nu_{\rm 3D}}{2R^2}\right]\mathrm{d}A_{\rm def} + \iint \frac{6}{d^2}\left[(1-\nu_{\rm 3D})\,\mathrm{Tr}\left(\epsilon^2\right) + \nu_{\rm 3D}\,(\mathrm{Tr}\,\epsilon)^2\right]\mathrm{d}A_{\rm init}\right\}. \tag{C.2}$$

References

1. G.M. Whitesides, Nature **442**, 368 (2006).
2. R. Seemann, M. Brinkmann, T. Pfohl, S. Herminghaus, Rep. Prog. Phys. **75**, 016601 (2012).
3. S. Kuriakose, P. Dimitrakopoulos, Phys. Rev. E **84**, 011906 (2006).
4. S.S. Datta, S.-H. Kim, J. Paulose, A. Abbaspourrad, D.R. Nelson, D.A. Weitz, Phys. Rev. Lett. **109**, 134302 (2012).
5. L. Landau, E.M. Lifschitz, *Theory of elasticity*, 3rd ed. (Elsevier Butterworth-Heinemann, Oxford, 1986).
6. M. Ben Amar, Y. Pomeau, Proc. R. Soc. London, Ser. A **253**, 411 (1997).
7. W. Helfrich, Z. Naturforsch. C **28**, 693 (1973).
8. C.I. Zoldesi, C.A. van Walree, A. Imhof, Langmuir **22**, 4343 (2006).
9. T.A. Kolesnikova, A.G. Skirtach, H. Möhwald, Expert Opin. Drug Deliv. **10**, 47 (2013).
10. A. Fery, R. Weinkamer, Polymer **48**, 7221 (2007).
11. S. Meille, E.J. Garboczi, Modelling Simul. Mater. Sci. Eng. **9**, 371 (2001).
12. F. Quéméneur, C. Quilliet, M. Faivre, A. Viallat, B. Pépin-Donat, Phys. Rev. Lett. **108**, 108303 (2012).
13. K. Brakke, Exp. Math. **1**, 141 (1992), or Surface Evolver Documentation: `http://www.susqu.edu/brakke/`.
14. J. Lidmar, L. Mirny, D.R. Nelson, Phys. Rev. E **68**, 0519010 (2003).
15. H.-T. Jung, S.Y. Lee, E.W. Kaler, B. Coldren, J.A. Zasadzinski, Proc. Nat. Acad. Sci. U.S.A. **99**, 15318 (2002).
16. H.S. Seung, D.R. Nelson, Phys. Rev. Lett. E **38**, 1005 (1988).
17. A. Sakashita, N. Urakami, P. Ziherl, M. Imai, Soft Matter **8**, 8569 (2012).
18. R. Mukhopadhyay, G. Lim, M. Wortis, Biophys. J. **82**, 1756 (2002).
19. W. Wintz, H.-G. Döbereiner, U. Seifert, Europhys. Lett. **33**, 403 (1996).
20. C. Quilliet, Eur. Phys. J. E **35**, 48 (2012).
21. S. Komura, K. Tamura, T. Kato, Eur. J. Phys. E **18**, 343 (2005).
22. H.-G. Döbereiner, E. Evans, I. Kraus, U. Seifert, M. Wortis, Phys. Rev. E **55**, 4458 (1997).
23. P.A. Kralchevsky, T.D. Gurkov, K.J. Nagayama, J. Colloid Interface Sci. **180**, 169 (1996).
24. J. Israelachvili, *Intermolecular & surface forces*, 2nd ed., section 17.8 (Academic Press, 2007).
25. W.K. Kegel, J. Groenewold, Phys. Rev. E **80**, 030401 R (2009).
26. F.I. Niordson, *Shell theory* (Elsevier, Amsterdam, 1985).
27. W. Pietraszkiewicz, Arch. Mech. **26**, 221 (1974).